Mesurer des déplacements ET des contraintes par correlation mécanique d'images

J. RÉTHORÉ[a], A. LEYGUE[a], M. CORET[a], L. STAINIER[a], E. VERRON[a]

a. Institut de Recherche en Génie Civil et Mécanique (GeM) – Ecole Centrale de Nantes, Université de Nantes, CNRS : UMR 6183 – 1, rue de la Noë BP92101 44321 Nantes cedex 3, France

Résumé :

Depuis ses premiers développements, la corrélation d'images a suscité un engouement très fort dans la communauté de la mécanique expérimentale. La possibilité d'accéder à la mesure d'un champ de déformation hétérogène offre en effet des perspectives nombreuses. Néanmoins, l'établissement d'une relation avec les contraintes ne peut être réalisé que dans des configurations où une solution analytique est connue. Ceci limite donc a priori la portée de l'approche aux cas où le champ de contrainte est homogène et aux cas où l'on peut supposer le comportement élastique et disposer d'une solution analytique (fissure, essai brésilien par exemple). Si l'on sort de ce cadre, il est nécessaire de recourir à la simulation numérique. En couplant mesure de champs par corrélation d'images et simulation numérique, on peut accéder au champ de contraintes. Cela suppose de connaître la loi de comportement du matériau. Mais on peut alors ajuster les paramètres de cette loi pour minimiser l'écart entre mesure et simulation. Cette approche est prometteuse mais elle suppose l'écriture d'une loi de comportement pour le matériau étudié ce qui peut parfois être limitant. On propose ici un nouvelle approche qui permet à partir d'images, d'accéder au champ de contrainte sans a priori sur le comportement. Cela repose sur une paramétrisation du déplacement adéquate en termes de contraintes. En plus, du champ de contrainte, on accède à un champ de déformation anélastique mesurant l'écart à la compatibilité vis-à-vis d'une déformation élastique dérivée du champ de contrainte. Des résultats illustreront les possibilités de la méthode par des exemples.

Abstract :

Since the pioneering works on digital image correlation, a huge effort has been devoted to the elaboration of strategies coupling measurements with numerical simulations. The main issue achieved with such coupling is the identification of constitutive law parameters using heterogeneous strain/stress fields experimental configurations. The main limitation of this framework is that a constitutive law is to be postulated, what sometimes reveals far from being straightforward. To circumvent this limitation, a methodology is proposed to build a parametric description of the displacement field for DIC which parameters are directly related to local stress and strain. With no assumption on the constitutive relation, the method allows for measuring displacement, strain but also stress fields. The ability of the method to measure stress fields is illustrated for different situations.

Mots clefs : corrélation d'images numériques, identification

Introduction

Since the pioneering work of Lucas, Kanade and others [1], image registration or Digital Image Correlation (DIC) has been widely used and developed in many ways. For mechanical experimentalists, the purpose of DIC is to measure displacement fields by comparing digital images of the sample under two different loading states. Sub-set based techniques are the most popular ones (see for example [2]) because they are the techniques implemented in commercial softwares. One should also mention the non-parametric formulation proposed by [3] that allows for measuring a displacement field pixel-wise. Compared to the conventional experimental methodology for constitutive behaviour analysis, which consists in performing uni-axial homogeneous stress/strain tests, DIC has the major advantage to provide for full displacement and strain fields. While this is useful to assess the quality of conventional tests, making good use of the rich data extracted from DIC measurements is still the purpose of many research works. One of the main issues is that the stress field in heterogeneous state configurations cannot be accessed without coupling measurements with numerical simulations.

Full-field measurements could be used on heterogeneous states configuration to enrich material state databases with more complex configurations. However, the stress analysis of complex tests requires the coupling with FE simulations that need a constitutive model. This is disappointing to observe that these two advanced methods (one that extracts material data from experiments and the other that makes use of material state data to perform simulations) cannot help each other. At this point, one ends up with the following fundamental question :

Is it possible to measure stress fields ?

In general, it has not yet been possible. There exist some optical techniques like photo-elasticity, caustics, or more recently Diffraction Computed Tomography, that allow to measure elastic stress fields but non-elastic stress evaluation is out of their scope. The aim of this paper is a proposition that may answer this question. It is not claimed that stress may become observable but we propose herein to formulate DIC so that strain but also stress fields can be directly estimated with no assumption on the constitutive relation. Plus, a supplementary information is obtained that can be interpreted as an internal variable field that measures the distance between the actual local constitutive equation and linear elasticity according to a given but arbitrary elastic tensor. The method will be referred to as Mechanical Image Correlation (MIC) as it allows to measure from digital images the local mechanical state of a material.

In the next Section, the principle of MIC are provided. In the last Section, some examples assessing the feasibility of the method and illustrating its potential are presented.

Mechanical Image Correlation (MIC)

Formulation

Let $\mathcal{C}$ be an elastic operator. Then, an elastic solution $\mathbf{u}_o, \boldsymbol{\sigma}_o$ according to $\mathcal{C}$ and balancing the measured load F_o is computed using a standard finite element solver. The vector collecting the nodal displacements of this elementary solution is denoted by $\mathbf{U}_o$. Without loss of generality, the actual displacement is written as

$$\mathbf{u} = \mathbf{u}_o + \bar{\mathbf{u}}. \tag{1}$$

$\bar{\mathbf{u}}$ results from the gap between the actual constitutive behaviour of the material (locally) and elasticity according to $\mathcal{C}$. As $\mathbf{u}_o, \boldsymbol{\sigma}_o$, balances the external load F_o, then it is concluded that the stress field $\bar{\boldsymbol{\sigma}}$, which is the gap between the actual stress field $\boldsymbol{\sigma}$ and $\boldsymbol{\sigma}_o$, from which $\bar{\mathbf{u}}$ derives, is a self-balanced stress field. It admits the following properties :

$$\text{div}\bar{\boldsymbol{\sigma}} = 0 \text{ over the ROI}, \quad \bar{\boldsymbol{\sigma}}\mathbf{n} = 0 \text{ over the boundary of ROI} \tag{2}$$

Using $\mathcal{C}$, an elastic strain $\bar{\boldsymbol{\varepsilon}}_e$ is obtained from $\bar{\boldsymbol{\sigma}}$. This strain may not fulfill the strain compatibility equation in general and the actual strain $\bar{\boldsymbol{\varepsilon}}$ derived from $\bar{\mathbf{u}}$ is thus written as

$$\bar{\boldsymbol{\varepsilon}} = \bar{\boldsymbol{\varepsilon}}_e + \bar{\boldsymbol{\varepsilon}}_a, \tag{3}$$

where $\bar{\boldsymbol{\varepsilon}}_a$ is an anelastic strain field accommodating strain compatibility constraint. Within this context, $\bar{\mathbf{u}}$ is a function of a self-balanced stress field $\bar{\boldsymbol{\sigma}}$ and an anelastic strain field $\bar{\boldsymbol{\varepsilon}}_a$. If Equation (2) is rewritten using Equation (3), one obtains :

$$\text{div}(\mathcal{C}\bar{\boldsymbol{\varepsilon}}) - \text{div}(\mathcal{C}\bar{\boldsymbol{\varepsilon}}_a) = 0 \text{ over the ROI}, \quad (\mathcal{C}(\bar{\boldsymbol{\varepsilon}} - \bar{\boldsymbol{\varepsilon}}_a))\mathbf{n} = 0 \text{ over the boundary of ROI} \tag{4}$$

This is a similar problem ones has to solve for thermo-elasticity, or for elasticity with volume forces. If $\bar{\boldsymbol{\varepsilon}}_a$ is given then $\bar{\mathbf{u}}$ is the solution of a linear elastic problem. There exists three types of $\bar{\boldsymbol{\varepsilon}}_a$ fields :

I the elastically associated stress field $\mathcal{C}\bar{\boldsymbol{\varepsilon}}_a$ is self-balanced. In this case the volume forces in Equation (4) vanish and because the computation of $\bar{\mathbf{u}}$ relies on an elastic problem, the trivial solution $\bar{\mathbf{u}} = \mathbf{0}$ is obtained.

II $\mathcal{C}\bar{\boldsymbol{\varepsilon}}_a$ is not self-balanced but $\bar{\boldsymbol{\varepsilon}}_a$ is compatible, *i.e.* there exists a displacement $\bar{\mathbf{u}}_a$ such that $\bar{\boldsymbol{\varepsilon}}_a$ is its symmetric gradient ($\bar{\boldsymbol{\varepsilon}}_a = \nabla^S \bar{\mathbf{u}}_a$). In this case $\bar{\boldsymbol{\varepsilon}} = \bar{\boldsymbol{\varepsilon}}_a$ and thus $\bar{\boldsymbol{\varepsilon}}_e = 0$. This means that $\bar{\boldsymbol{\sigma}}$ vanishes and $\bar{\mathbf{u}} = \bar{\mathbf{u}}_a$ derives from a compatible strain field.

III $\mathcal{C}\bar{\boldsymbol{\varepsilon}}_a$ is neither self-balanced nor compatible. In this case $\bar{\boldsymbol{\varepsilon}}$ is different from $\bar{\boldsymbol{\varepsilon}}_a$ and $\bar{\boldsymbol{\sigma}}$ does not vanish.

Type I fields has no effect on $\bar{\mathbf{u}}$. But type II and III fields produce an additional displacement for which one has to propose a parametrization. This is the purpose of the next two paragraphs.

Type II anelastic fields are such that $\mathcal{C}\bar{\boldsymbol{\varepsilon}}_a$ is not self-balanced but $\bar{\boldsymbol{\varepsilon}}_a$ is compatible. As a consequence, $\bar{\mathbf{u}}$ is solution of an elasticity problem with volume forces deriving from a compatible strain field and $\bar{\boldsymbol{\varepsilon}}_a = \bar{\boldsymbol{\varepsilon}}$. Numerically, it is convenient to generate a set of elastic solution for this problem from the eigen modes of the elastic finite element stiffness matrix. This set of eigen modes is stored in matrix format as $\mathbf{U}_{II}$. In this case the set of anelastic fields is $\mathbf{E}_{aII}$ that is the symmetric gradient of $\mathbf{U}_{II}$ components.

Type II anelastic fields are such that $\mathcal{C}\bar{\boldsymbol{\varepsilon}}_a$ is not self-balanced but $\bar{\boldsymbol{\varepsilon}}_a$ is compatible. As a consequence, $\bar{\mathbf{u}}$ is solution of an elasticity problem with volume forces deriving from a compatible strain field and $\bar{\boldsymbol{\varepsilon}}_a = \bar{\boldsymbol{\varepsilon}}$. Numerically, it is convenient to generate a set of elastic solution for this problem from the eigen modes of the elastic finite element stiffness matrix. This set of eigen modes is stored in matrix format as $\mathbf{U}_{II}$. In this case the set of anelastic fields is $\mathbf{E}_{aII}$ that is the symmetric gradient of $\mathbf{U}_{II}$ components.

Resolution

Based on the construction of these bases, the parametrization of the displacement $\mathbf{u}$ is achieved. The first component of this parametrization is $\mathbf{U}_o$. This displacement vector is obtained from a FE elastic

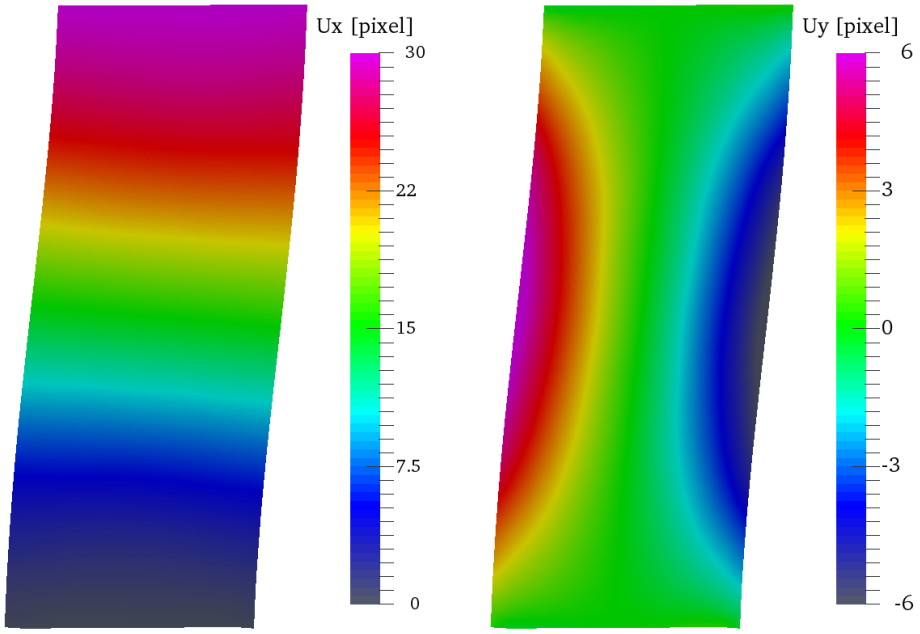

(a) (b)

FIGURE 1 – Horizontal and vertical displacement (in pixel) by MIC analysis for the linear isotropic test case.

simulation using $\mathcal{C}$ as the elastic tensor and a prescribed displacement measured by DIC along the boundary of the ROI where non-zero stress conditions apply. The amplitude of this displacement is adjusted so that the resulting forces F_o matched the experimental data. Note that because $\mathcal{C}$ may not be the actual constitutive operator, after adjustment of F_o, the displacement along the boundary of the ROI does not match the measured displacement anymore.

The next terms of the displacement parametrization are obtained from the anelastic fields, namely $\mathbf{U}_{II}$ and $\mathbf{U}_{III}$. This parametrization does not contain rigid body motions (two translations and one rotation in 2D) that are considered through additional basis vectors $[\mathbf{U}_R]$. These two bases are then concatenated as $[\bar{\mathbf{U}}] = [\mathbf{U}_{II}\mathbf{U}_{III}\mathbf{U}_R]$ for describing $\bar{\mathbf{u}}$.

The optical flow equation

$$f(\mathbf{x}) - g(\mathbf{x} + \mathbf{u}(\mathbf{x})) \tag{5}$$

is solved using the parametrization proposed above. DIC provides for the amplitude of $[\bar{\mathbf{U}}]$ components, let us say $\bar{\Lambda}$. This of course gives a direct access to the measured displacement and total strain field. In a post-processing step, anelastic strain field $\bar{\boldsymbol{\varepsilon}}_a$ is derived from $\mathbf{E}_{aII}$, $\mathbf{E}_{aIII}$ and the corresponding components of $\bar{\Lambda}$. The stress field is then reconstructed from $\boldsymbol{\sigma}_o$ derived from $\mathbf{u}_o$ and $\bar{\boldsymbol{\sigma}}$ that is derived from the additional elastic strain $\bar{\boldsymbol{\varepsilon}}_e = \bar{\boldsymbol{\varepsilon}} - \bar{\boldsymbol{\varepsilon}}_a$.

Examples

Isotropic linear elasticity

In this example, the model consists in a rectangular domain of 1400×3500 pixels. In the FE simulation used for generating the synthetic data, the displacement along the bottom edge is clamped while along the

top edge, the vertical displacement is set to 0 but the horizontal displacement is prescribed to 30 pixels. In this numerical simulation the material is assigned a linear isotropic behaviour defined by its Young's modulus and Poisson's ratio set to 5 GPa and 0.2 respectively.

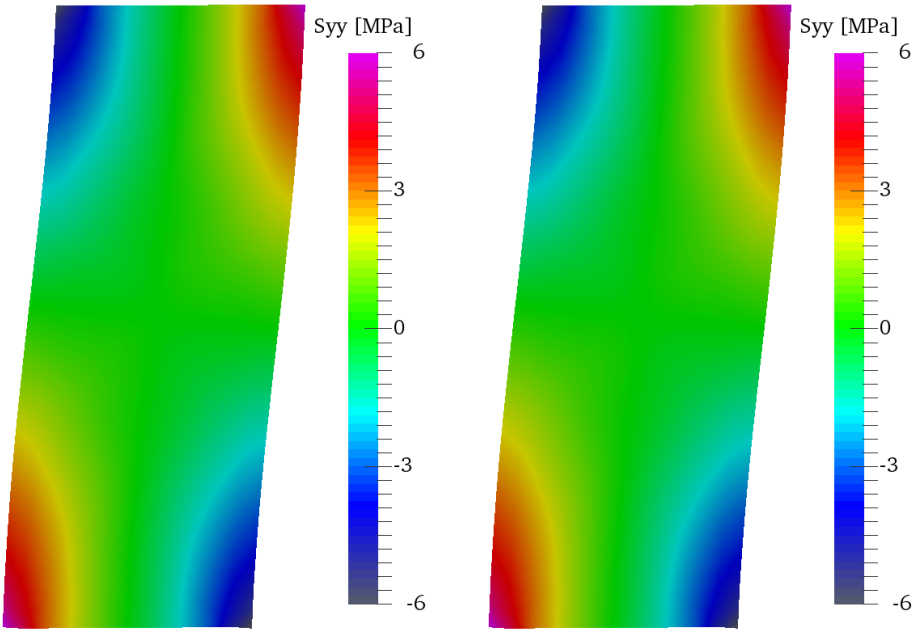

(a) (b)

FIGURE 2 – Vertical stress field (in MPa) for the linear isotropic test case : (a) FE simulation used to generate the synthetic image, (b) MIC analysis.

For the MIC analysis, where only type II fields are used, these material parameters are changed so that $\mathcal{C}$ differs from the actual elastic tensor. They are set to 2.5 GPa and 0.1 respectively. A mesh of triangular elements of 96-pixel size is used and 100 modes are considered for each anelastic strain field bases. Displacement fields obtained from this analysis are depicted in Figure 1. They are almost identical to the displacement field obtained by DIC and to the one that is used to generate the deformed image. To assess the accuracy of the stress field measurement, the measured stress component in the vertical direction is compared to its homologous field in the numerical simulation in Figure 2. It is worth noting that there is a very good agreement between the measurement and the actual values of stress. To further demonstrate how the actual constitutive law is retrieved from the MIC analysis, the spherical and deviatoric parts of the stress tensor are plotted against their strain counterpart in Figure 3. It is obtained that a linear regression in the cloud of material state points obtained by MIC would allow for retrieving the actual elastic constants.

Residual stress

In this example, the same geometry as in the previous one is considered. The material is assigned the same properties. The FE simulation is run to simulate the existence of a remaining elasto-plastic strain field. To make this remaining strain not compatible, only its yy component is considered and a linear evolution along x from -0.0025 to 0.0025 is assigned. An elastic problem is solved under the volume forces generated by this residual strain and the deformed image is generated by using the resulting displacement field. In Figure 4, the measured and prescribed displacement are compared. A good agreement

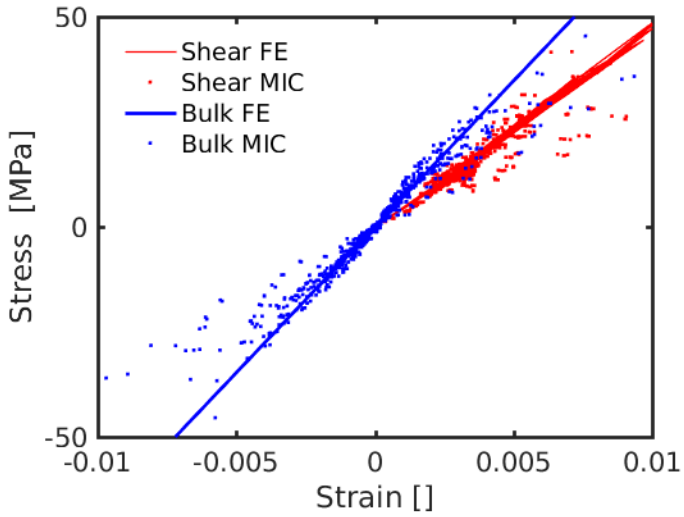

FIGURE 3 – Stress *v.s.* strain spherical and deviatoric components : comparison between FE simulation and MIC measurement.

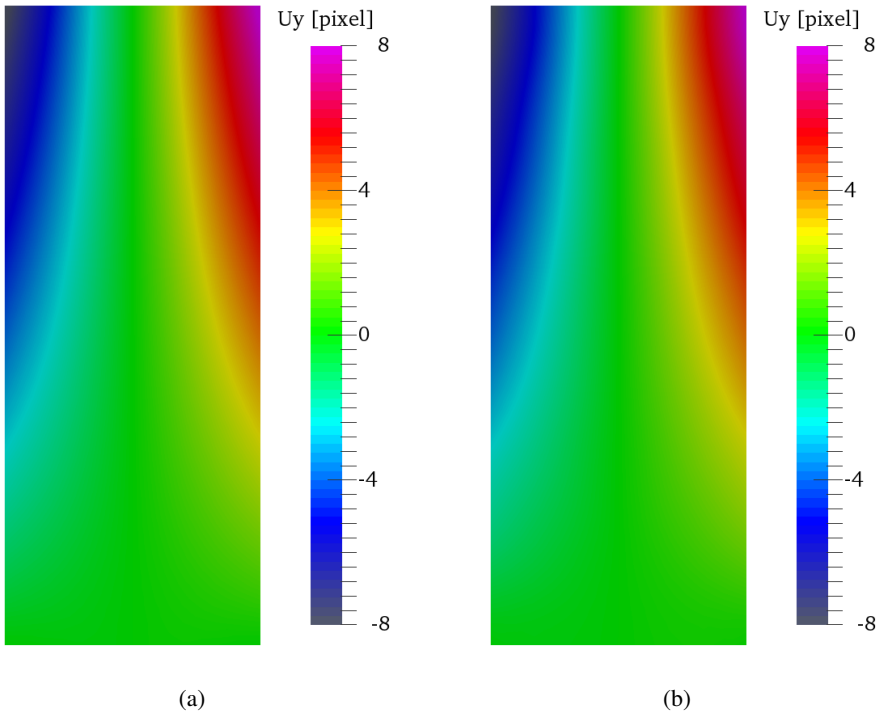

(a) (b)

FIGURE 4 – Comparison of the horizontal displacement (in pixel) from the FE simulation (a) and measured by MIC for the test case with residual stress.

is obtained. This is confirmed in Figure 5 which compares prescribed and measured fields of vertical anelastic strain and stress respectively. For plotting these curves, the element wise values of the fields have been re-interpolated on a regular grid and then averaged along the y direction. The residual strain distribution is retrieved almost perfectly by MIC. The residual stress measurement is slightly less accurate but one has to point out that this residual stress level derive from elastic strain lower than 0.0001 (far below the usual resolution of DIC).

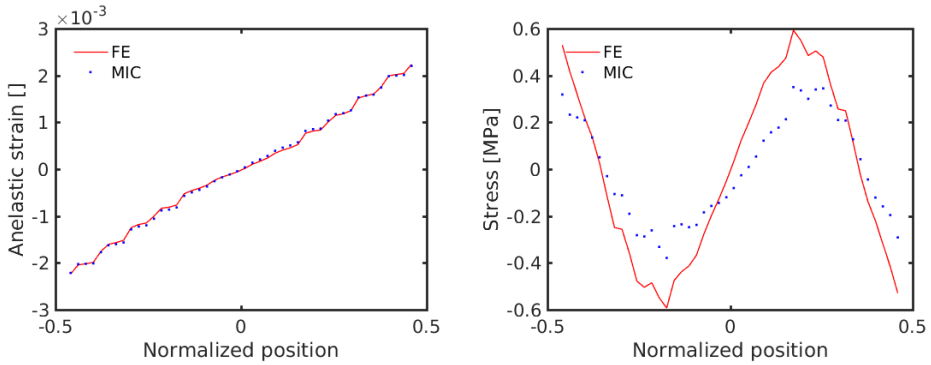

(a) (b)

FIGURE 5 – Comparison of yy component of the anelastic strain (a) and residual stress (b) from the FE simulation and measured by MIC for the test case with residual stress.

Conclusion

A methodology is proposed to build a parametric description of the displacement field for DIC which parameters are directly related to local stress and strain. With no assumption on the constitutive relation, the method allows for measuring displacement, strain but also stress fields. Further, an anelastic strain field measuring the *distance* between the actual local constitutive behaviour and elasticity according to a given but arbitrary elastic tensor is obtained. The ability of the method to measure stress fields in different situations is illustrated. The raw data extracted from the measurement are admissible material states in a space of dimension 9 for 2D problems.

Acknowledgments

The support of Région Pays de la Loire and Nantes Métropole through grant Connect Talent IDS is gratefully acknowledged.

Références

[1] Bruce D Lucas, Takeo Kanade, et al. An iterative image registration technique with an application to stereo vision. In *IJCAI*, volume 81, pages 674–679, 1981.

[2] MA. Sutton, M. Cheng, WH. Peters, YS. Chao, and SR. McNeill. Application of an optimized digital image correlation method to planar deformation analysis. *Image Vision Computing*, 4(3) :143–150, august 1986.

[3] T Vercauteren, X Pennec, A Perchant, and N Ayache. Diffeomorphic demons : Efficient non-parametric image registration. *NeuroImage*, 45(1) :S61–S72, 2009.